HEMANT KUMAR
DEBASIS DEB
and
DEBASHISH CHAKRAVARTY

Analysis of the vertical movement of crown pillar in cut and fill mining using finite element method

Crown pillar is a horizontal pillar left to protect the upper level workings when stope advances along the up dip direction and approaches to the upper level in cut and fill method of mining. These horizontal pillars are the main support structures for stopes during excavation. In this study the vertical movement of the pillars at crown level has been analysed by varying the rock mass parameters such as geological strength index (GSI), uniaxial compressive strength (UCS or fãci), modulus of elasticity (E), depth of pillar from surface (D) and thickness of horizontal pillar (T) using finite element method.These analyses have been conducted based on 135 non-linear numerical models considering Drucker-Prager failure criterion in plane strain condition. Results of finite element models are represented in terms of displacements in rock mass of the pillars. Displacement profiles of rock mass along the predefined paths are obtained, presented and analyzed for different models having variation in geo-mining conditions. Finally, the most important parameters affecting the convergence significantly are identified which may be incorporated in the design of the optimum crown pillar thickness.

Keywords: Geo-mining parameters, crown pillar; numerical modelling; vertical displacement, FEM, orebody width, pillar depth.

1. Introduction

In cut and fill method of stoping in underground metal mining, horizontal pillars are left at suitable level intervals to provide the base of the backfilled material as well as to support the hanging wall and footwall of the stope after exploitation of the minerals. Horizontal pillars at each level consist of level drive. Horizontal portion above the level drive is known as sill pillar and horizontal portion below the level drive is known as crown pillar (as per the Indian metal mining practices) as shown in Fig.1. Crown pillars are left to protect the upper level drive and jointly the sill and crown pillar known as horizontal pillar protect all the working above this horizontal pillar. These horizontal pillars are the main support

Messrs. Hemant Kumar, Department of Mining Engineering, IIT (ISM) Dhanbad 826 004 and Debasis Deb and Debashish Chakravarty, Department of Mining Engineering, IIT, Kharagpur 721 302, India

structures for stopes during excavation and after excavation throughout the life of the mine. Although a thick sill and crown pillar provide support for the hanging wall and add to the overall stability of the stopes, it may be uneconomic from mineral conservation point of view. Thus the optimization of sill and crown pillar dimension is very important for metalliferous mines [1].

Stability of structures in deep underground mines can be broadly divided into three different categories; global, regional and local depending on volume of rock involved [2]. The major factors which play important role in pillar stability are, effect of depth of cover [3], effect of size of excavation [4, 5], effect of rock mass properties [4, 5], effect of backfilling [6, 7], effect of reinforcement [8], effect of horizontal stress [2, 5], and effect of the dipping [9].

This study analyzes the vertical rock/pillar movement in stope regimes using two dimensional numerical techniques by varying geo-mining conditions such as rock geological strength index (GSI), uniaxial compressive strength (UCS or fãci), modulus of elasticity (E), depth of pillar from surface (D) and thickness of horizontal pillar(T). These analyses have been conducted based on 135 non-linear numerical models considering Drucker-Prager material model in plane strain condition. Results of finite element models are represented in terms of displacements in rock mass of the pillars. Displacement profiles of rock mass along the predefined paths are obtained, presented and analyzed for different models having variation in geo-mining conditions. Finally, the most important parameters affecting the convergence significantly are identified. Thus, identified parameters can be used for further design of the optimum crown pillar thickness.

2. Case study mine and models parameters

The orebody of the case study mine has varying dip as well as width as shown in Fig. 2. Finite element models of the stopes and pillars are developed below 596 mL indicating level intervals at 685 mL, 815 mL, 750 mL, and 880 mL. The meshed model with loading conditions and the in-situ models are developed considering the actual dip of the orebody, thickness of orebody at different levels and levels at designated depth. It is noticed that an excavated height of
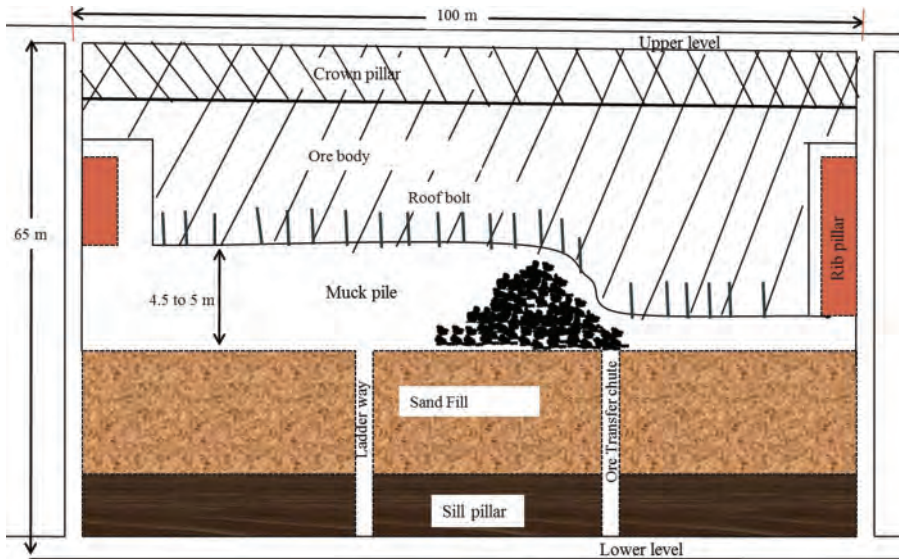
Fig.1 A typical longitudinal section of cut and fill stope (after Kumar, et al., 2015)
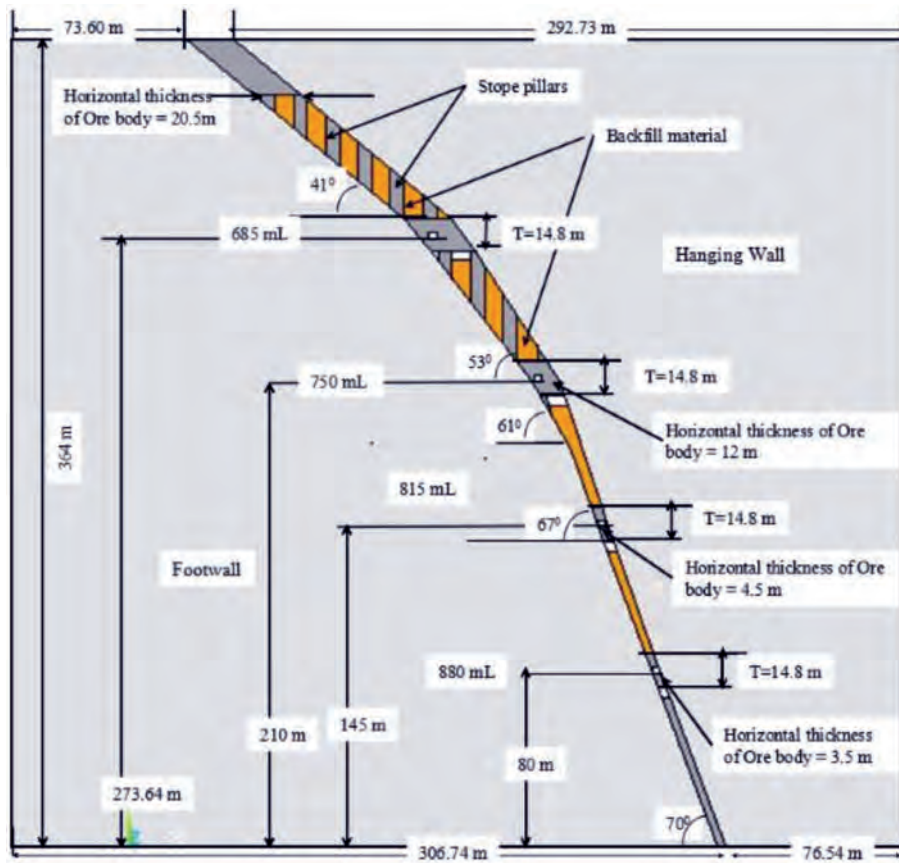

Fig.2 Geometric model of the case study mine (after Kumar, et al., 2015)

horizontal pillars of 14.8 m ($6 \times 2 + 2.8$) are left considering level drive of height 2.8 m. Similarly, separate solid models are developed to represent a horizontal pillar thickness of 10.8 m, 12.8 m, and 16.8 m keeping all other dimensions same as first model. This variation in geometrical model has been done to analyze the stability of horizontal pillar with variation of other parameters viz. depth of mining, rock mass conditions and others [1]

3. Geotechnical study of case study mine

Geotechnical study shows that the variation in GSI of the orebody rock mass ranges between 42 and 75, uniaxial compressive strength lies between 46.23 MPa and 86.73 MPa, and modulus of rigidity ranges between 9.43 GPa and 16.22 GPa. The GSI is a practical system and depends on the visual impression of the rock structure to estimate the strength of rock mass. GSI value lies in the range of 0–100 as in the case of RMR and is calculated from charts based on the quality of the rock structure and the condition of the rock surfaces [10]. These data suggest variation in strength properties of the rock mass and hence accordingly this study guides wide range of rock properties as modelling parameters. Three variations of GSI are considered for the study, viz., 50, 60 and 70. Similarly, the uniaxial compressive strength (UCS) of orebody is varied as 50, 65 and 75 MPa, modulus of elasticity of intact rock is varied as 10, 15 and 20 GPa. The strength and modulus of rigidity of rock mass are estimated based on UCS, E, GSI and m_i (Hoek and Brown parameter). Altogether, 108 finite element models have been developed, based on all possible interactions [namely, modulus of orebody (3) × thickness of horizontal pillar (4) × RMR/GSI of orebody (3) × uniaxial compressive strength (3)]. Apart from this, 27 in-situ or pre-mining finite element models are also developed by varying rock mass parameters. These models are analyzed in plane strain conditions considering non-linear material behaviour based on Drucker-Prager failure criteria.

4.5 m is left after the last slice below the crown pillar to analyze the worst possible stress conditions and convergence of rock in the pillars. In levels 815 mL and 880 mL, post pillars (stope pillars) are not needed since width of the orebody is less than 8 m as suggested by the regulatory body in India. For example, if the thickness of sill and crown pillar is 6 m each,

3.1 PROPERTIES OF BACKFILL MATERIAL USED IN CASE STUDY MINE

Backfilling is one of the most important activity in cut and fill method of mining which provides the working platform as well as support to hangwall and footwall during stoping operations. It also facilitates the safe and selective extraction of ore from the stope. The backfill material used in the study mine is mill tailings of Young's modulus 500 MPa, density 1800 kg/m^3 and poisons ratio 0.3.

3.2 IN-SITU STRESS IN THE CASE STUDY AREA

The in-situ stress measurement results suggest a horizontal and vertical pressure of 10.14 Mpa at a depth of 596 m from the surface and gradient-horizontal pressure of 0.053 MPa/m.

The direction of the major horizontal stress is found to be N16º-N21º.

Fig.4 Finite element meshed model showing orebody, hanging wall, and footwall below 596 mL along transverse section A-A' before the excavation of mining area (after Kumar, et al., 2015)

4. Finite element models

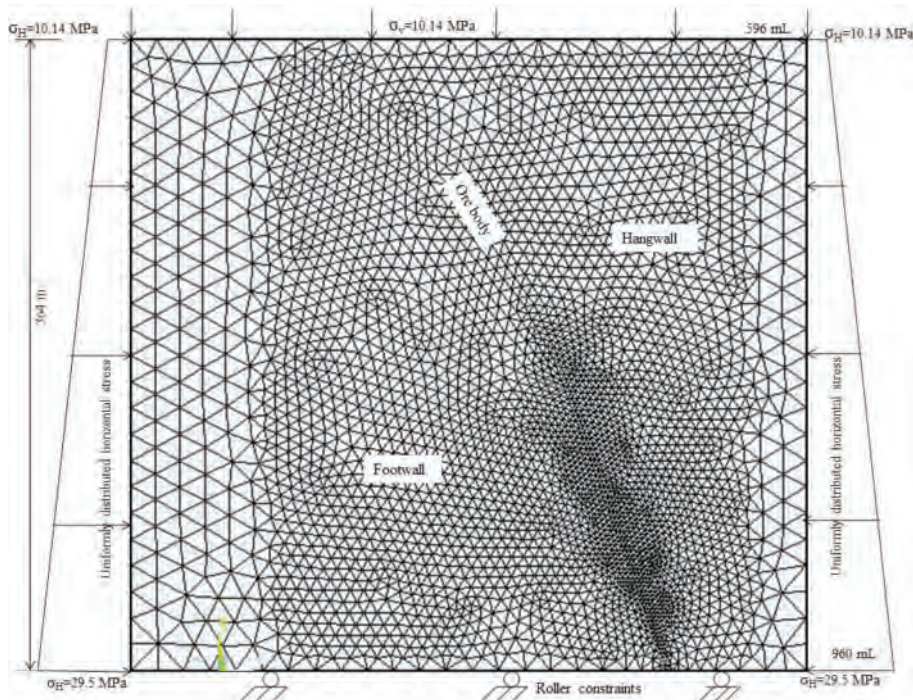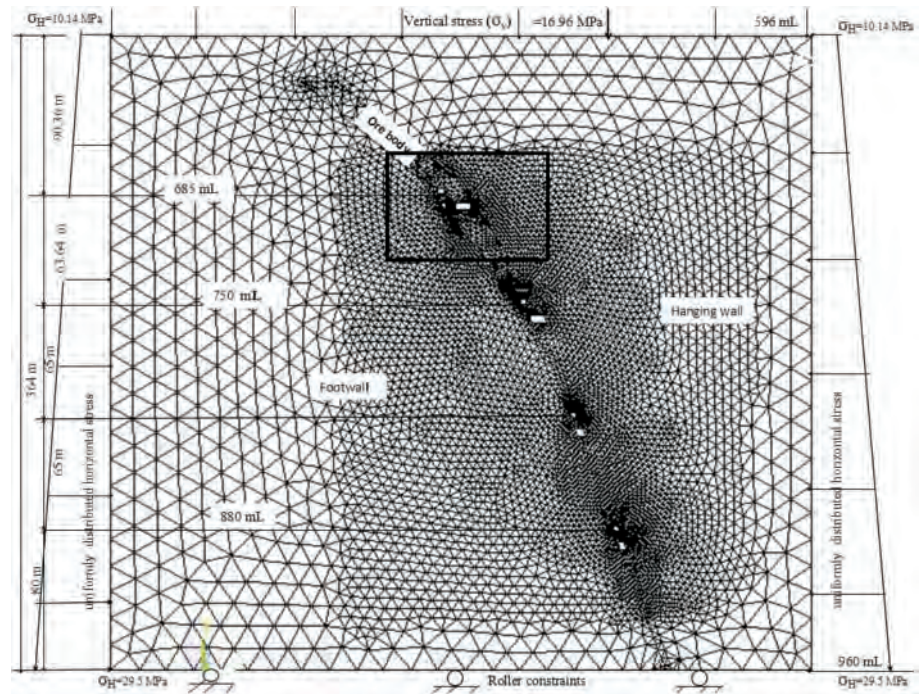Rock mass, orebody and openings are modelled with 6-noded quadratic triangular elements. These elements have two degrees of freedom at each node: translations in coordinate axes, i.e. x and y directions. The finite element model of case study mine represents the vertical transverse-section along, approximately the middle portion of W$_4$ stope block and hence, plane strain constitutive material behaviour is assumed. It is important to note that this model resembles the final stage of stoping operation where maximum ore recovery has been done between levels, and stope above is approximately filled with backfill material.

4.1 MESHED IN-SITU MODEL

Fig.3 shows the meshed view of in-situ model developed for the analysis of stress, strain and displacement of rock mass prior to excavation or mining. In-situ models provide the ideas about stress and displacement of rock mass prior to mining or excavation. Openings or excavation in rock mass causes re-orientation of stress regime and change in displacement in the rock mass. A total of 27 (3 variation of GIS × 3 variation of UCS × 3 variation of modulus of rigidity, E) in-situ finite element models are developed by varying the material properties of rock mass. An additional pressure of 16.98 MPa is applied uniformly on the top of

Fig.3 In-situ finite element meshed model showing orebody, hanging wall, and footwall below 596 mL along transverse section A-A' before the excavation of mining area

the model to consider the pressure of overlying strata. A gradient-horizontal pressure 0.053 MPa/m is applied from left to right and also from right to left the in meshed in-situ model (Fig.3).

The solid models as well as the finite element meshes are developed using ANSYS software tool as shown in Fig.4. The bottom boundary of the models is roller-constrained. A uniform load distribution of gradient 0.053 MPa/m is applied on the sides to simulate the in-situ stress condition of the mine. The meshing of complete model of 6 m sill/crown pillar thickness produced an average of 12081 6-noded triangular elements and 24439 nodes. A quadratic triangular element consists of 6 nodes is mostly suitable for two dimensional (2D) stress analysis with material non-linearity. In general, finer mesh is developed in the stoping zone for better evaluation of displacements, stresses and strains. Coarse mesh is developed in the rock mass away from the mining effected zones.

5 Analysis of vertical movement of rock mass of crown pillar

In this study the analysis of the vertical displacement of roof is carried out for two main purposes:

(i) To analyze the variations of vertical movement of the roof of the stope under various geo-mining conditions, and

(ii) To identify the most significant parameters affecting the roof convergence in horizontal pillar in cut and fills mining which can be incorporated for further investigation into the design of optimum horizontal pillar thickness.

It has been mentioned earlier that after taking the final slice in a horizontal cut and fill stope, generally 4.5 m height of
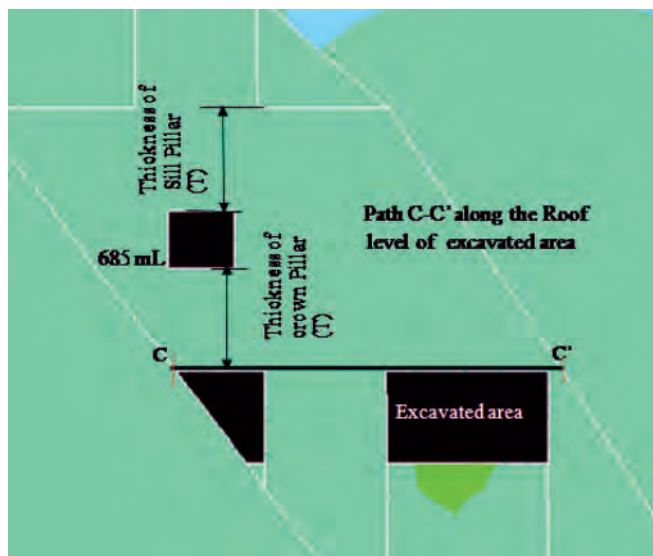

Fig.5 Zoomed view of 685 mL showing the path C-C' on which vertical movement of rock has been analyzed

excavated area remain open or unfilled for duration of approximately 15 to 30 days till final backfilling operation begins. In addition, experience gained from working in the study mine suggests that for all practical situations, 0.5 to 1.0 m of the final excavated height remain unfilled even after the completion of backfilling in the stope. This may happen due to inconvenience of backfilling at low height and/or settlement of sand after water is drained out. In any case, a vertical movement of roof strata is imminent in case of horizontal cut and fill method of stoping.

In this case, displacement profiles of rock mass along the path C-C' as shown in Fig.5 are obtained, presented and analyzed for different models having variation in geo-mining conditions viz., pillar thickness (T), GSI, UCS (sci), modulus of elasticity (E) and depth of workings (D). In-situ displacements are subtracted from those of excavated models along the same path C-C' to analyze the effect of excavations and material yielding on vertical displacement fields.

Fig.6 shows the variations of vertical displacement of orebody along C-C' path for different pillar thicknesses and geo-mining conditions: GSI=70, UCS (sci)= 75 MPa, E = 15 GPa and D = 685 mL. From Fig.6 it can be observed that the maximum vertical displacement occurs above the excavated area and approximately middle of the excavated zone. Table 1
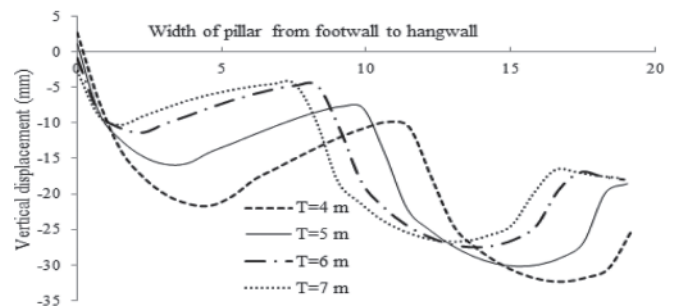

Fig.6 Vertical displacement of rock mass at the bottom level of crown pillar of thickness 4 m, 5 m, 6 m, and 7 m.(Geo-mining conditions: GSI = 70, UCS = 75 MPa, E = 15GPa, and D = 685 mL)
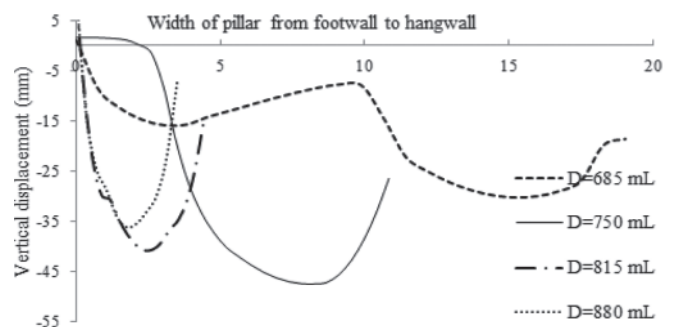

Fig.7 Vertical displacement of rock mass at the bottom level of crown pillar at depth 685 mL, 750 mL, 815 mL, and 880 mL. (Geo-mining conditions: GSI= 70, UCS=75 MPa, E= 15 GPa, and T= 5 m)

lists the maximum displacements obtained for different pillar thicknesses and the variation in convergence with the variation in pillar thickness. From this table, it can be seen that if pillar thickness is designed to be 4 m instead of 5 m, the maximum vertical displacement increases by 7.05%. Similarly, if pillar thickness changes from 5 m to 6 m or to 7 m the maximum vertical displacement decreases by 8.94% or 11.55% respectively. Similar pattern of results have been obtained from other models having values of GSI=50 and 60, UCS=50 MPa and 65 MPa, E =20 GPa and 10 GPa, and D = 750 mL, 815 mL and 880 mL. The extent and magnitude of displacements vary depending upon the depth of workings, width of pillars, GSI, UCS and modulus of elasticity (E).

5.2.2 Effect of depth of working on vertical displacements

The vertical displacement of rock mass along the path C-C' changes significantly with depth of workings. Fig.7 depicts the vertical displacement for different depths and it is clear that since width of the orebody and hence width of excavation is wider at 685 mL and 750 mL, the magnitude of vertical displacement is also high.

Table 2 lists the maximum vertical displacement at different depths of working and shows that this parameter has an increasing trend with depth of workings. From this table, it can be observed that with increase in depth of working from 685 mL to 750 mL, 685 mL to 815 mL, and 685 mL to 880 mL the vertical displacement increases by 57.07%, 34.94% and 19.70% respectively. Close view of the above data reveal that at greater depths (i.e. 815 mL and 880 mL) the maximum convergence values are less with respect to the convergence at upper levels (i.e. 685 mL and 750 mL). This decrease in convergence value can be explained in terms of decreasing width of excavations or orebody width otherwise it would have been the higher values. Similar pattern of results have been obtained from other models having values of GSI = 50 and 60, UCS = 50 MPa and 75 MPa, E = 20 GPa and 10 GPa, T = 4m, 6m, and 7m.

TABLE 1: VERTICAL DISPLACEMENT OF ROCK MASS AT THE BOTTOM LEVEL OF CROWN PILLAR FOR DIFFERENT PILLAR THICKNESS VALUES

T = Pillar thickness (m)	Vertical displacement of rock mass at the roof level of excavated area	
	Maximum (negative sign represents downward movement)	% change (negative sign represents the decrease in displacement)
4	-32.33	7.05
5	-30.20	0
6	-27.49	-8.94
7	-26.71	-11.55

TABLE 2: VERTICAL DISPLACEMENT OF ROCK MASS AT BOTTOM LEVEL OF CROWN PILLAR FOR DIFFERENT DEPTH OF WORKINGS

D = Pillar depth (m)	Vertical displacement of rock mass at the roof level of excavated area	
	Maximum (negative sign represents downward movement)	% change (increase in vertical displacement w.r.t 685 mL)
685 mL	-30.2	0
750 mL	-47.43	57.05
815 mL	-40.75	34.93
880 mL	-36.15	19.70

TABLE 3: VERTICAL DISPLACEMENT OF ROCK MASS AT BOTTOM LEVEL OF CROWN PILLAR FOR DIFFERENT VARIATION OF GEOLOGICAL STRENGTH INDEX (GSI)

GSI	Vertical displacement of rock mass at the roof level of excavated area	
	Maximum downward movement (negative sign represents downward movement)	% change (negative sign means decrease in vertical displacement)
50	-36.48	0
60	-32.53	-10.82
70	-30.20	-17.21

TABLE 4: VERTICAL DISPLACEMENT OF ROCK MASS AT BOTTOM LEVEL OF CROWN PILLAR FOR VARIATIONS OF MODULUS OF ELASTICITY (E)

E (GPa)	Vertical displacement of rock mass at the roof level of excavated area	
	Maximum downward movement (mm) (negative sign represents downward movement)	% change (negative sign means decrease in vertical displacement)
10	-36.26	6.06
15	-30.20	0
20	-28.52	-5.60

5.2.3 Effect of GSI on vertical displacements

GSI plays an important role in determining the onset of yielding of rock mass [11]. Hence, rock mass having lower GSI would yield more and produce higher displacements as compared to a rock mass having higher GSI. Fig.8 shows that keeping all the other parameters constant, vertical displacement of rock mass along the path C-C' is more if GSI of orebody is 50 as compared to 70. Considering GSI=50 as reference, Table 3 estimates that the maximum vertical displacement may decrease by 10.82% and 17.21% if GSI of orebody changes to 60 and 70 respectively. It may be noted that the magnitude of vertical displacement is as high as 36.48

mm for GSI = 50 and E = 15 GPa. For lower stiffness of orebody, magnitude of vertical displacement may further increase signifying occurrence of a possible roof/rock fall event. Similar results are obtained for other geo-mining conditions.

5.2.4 Effect of modulus of elasticity (E) on vertical displacement

It is expected that lower E values of rock mass would cause higher displacement around the excavations and this phenomenon is evident from Fig.9. This plot contains vertical displacement along C-C' path at 750 mL for GSI=70 and UCS=75 MPa. It shows that the maximum vertical displacement may reach up to 36.26 mm for E=10 GPa. This vertical displacement becomes significant in terms of roof fall if E value of orebody along with GSI reduces further at any location around the excavations. The change of the maximum displacement as estimated in Table 4 is about 5.6% if stiffness of orebody changes from 15 GPa to 10 GPa.

5.2.5 Effect of uni-axial compressive strength (UCS) (σ_{ci}) on vertical displacement

Similar to GSI, UCS of rock mass also determines the onset of yielding and hence controls the elasto-plastic behaviour of material. Fig.10 depicts that for lower $f$ãci, material yields more and hence higher displacement occurs at the roof level. A maximum displacement of about 33.12 mm is observed for excavation width of 8 m for the geo-mining conditions GSI= 70, E=15 GPa, D=685 mL, T= 5 m and UCS=50 MPa. Table 5 summarizes the magnitude of the maximum vertical displacement and their variations with respect to (UCS) $f$ãci. From this table, it can be ascertained that if strength of orebody changes from 50 MPa to 65 MPa, a decrease of about 6.7% is noted in the maximum vertical displacement. Similar results are obtained for other geo-mining condition.

6. Interpretation and conclusions

In the above analysis, five parameters are varied namely, thickness of pillar (T), depth of working (D), geological strength index (GSI), modulus of elasticity (E) and uniaxial compressive strength ($f$ãci) to determine the effect on vertical displacement at roof level. The following summary can be made based on the above discussions:

(1) The maximum vertical displacement at the bottom level of crown pillar is 30.20 mm for the geo-mining conditions GSI
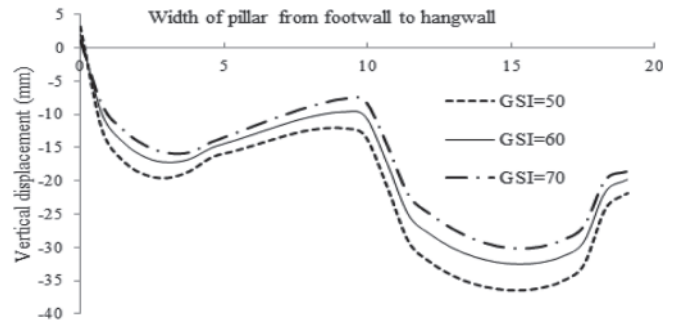

Fig.8 Vertical displacement of rock mass at the bottom level of crown pillar for different values of GSI=50, 60 and 70 (for UCS = 65 MPa, E = 15 GPa, D = 750 mL and T = 5 m)
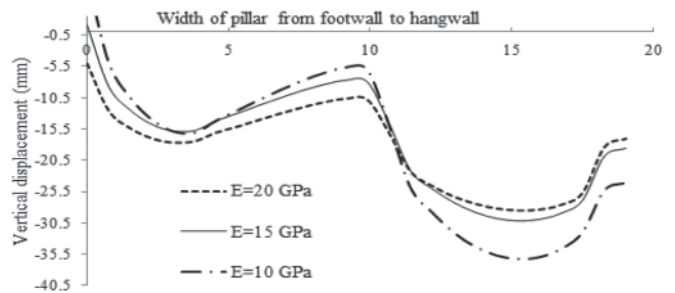

Fig.9 Vertical displacement of rock mass at the bottom level of crown pillar (Geo-mining conditions: UCS = 65 MPa, GSI = 60, D = 750 mL and T = 5 m)
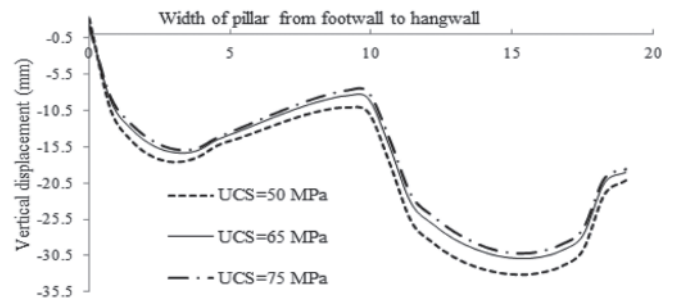

Fig.10 Vertical displacement of rock mass at the bottom level of crown pillar for different variations of UCS (Geo-mining conditions: GSI = 70, E = 15 GPa, D = 685 mL and T = 5 m)

= 70, σ_{ci} = 75 MPa, E = 15 GPa, T = 5 m and D = 685 mL. If the thickness of crown pillar decreases to 4 m instead of 5 m with same geo-mining conditions as above, the maximum vertical displacement can be seen to be 33.22 mm. If we analyze the same with GSI=50, keeping all the other geo-mining conditions unchanged, it has been observed that vertical displacement changes from 41.73 mm to 46.18 mm; and similar results are obtained for the other parameters as well. Hence, it can be said that thickness of pillar certainly effects the vertical movement of rock mass.

(2) From the above analysis it can also

TABLE 5: VERTICAL DISPLACEMENT OF ROCK MASS AT THE BOTTOM LEVEL OF CROWN PILLAR FOR DIFFERENT VARIATION OF UNIAXIAL COMPRESSIVE STRENGTH (σ_{ci})

σ_{ci} (MPa)	Vertical displacement of rock mass at the roof level of excavated area	
	Maximum downward movement (mm) (negative sign represents downward movement)	% change (negative sign means decrease in vertical displacement)
50	-33.12	0
65	-30.90	-6.70
75	-30.20	-8.81

be interpreted that the maximum variation in vertical movement of rock was observed with the variation of depth of workings. If the depth of working (D) increases to 750 mL from 685 mL with same geo-mining conditions as above, the maximum vertical displacement can be seen to be increased by 57.05%. However, above data reveal that at greater depths (i.e. 815 mL and 880 mL) the maximum convergence values are less with respect to the convergence at upper levels (i.e. 685 mL and 750 mL). This decrease in convergence value can be explained in terms of decreasing width of excavations or orebody width. Hence, the depth of working influences the most in the vertical movement of rock mass.

(3) Variations of GSI, T, σ_{ci} and E also effect significantly the vertical movement of rock mass of crown pillar. Next to the depth of working, GSI also plays very important role in the convergence of roof rock.

(4) From the above analysis it is observed that variations of GSI, has significant effect and variation of E, and σ_{ci} are less significant. Apart from GSI, E and σ_{ci}, it has also been observed that depth (D) influences most significantly the vertical movement of rock mass.

(5) Above analysis suggests that the rock lying in the roof level of excavated area is being affected significantly by each of the above parameters and can be incorporated for further investigation into the optimum horizontal pillar thickness (crown pillar + sill pillar). In few cases, if variation of modulus of rigidity (E) is small within the orebody, hanging wall and footwall, it may be ignored for the design of optimum pillar thickness.

References

1. Kumar, H., Deb, D. and Chakravarty, D. (2016): "Numerical Analysis of Sill and Crown Pillar Stability for Multilevel Cut and Fill Stopes in Different Geomining Conditions." *International Journal of Geotechnical and Geological Engineering*, Vol. 34, issue 2, pp 529–549.

2. Tavakoli, M. (1994): "Underground metal mine crown pillar stability analysis" University of Wollongong, (Research online) Unpublished Thesis collections.

3. Lu, T. K., Guo, B. H. and Cheng, L. C. (2009): "Review and interpretation of intersection stability in deep underground based on numerical analysis" Taylor & Francis Group, London; ISBN 978-0-415-48475-6.

4. Edelbro, C. (2003): "Rock Mass Strength – a review." *Technical Report Lulea University of Technology. Department of Civil Engineering Division of Rock Mechanics*. ISSN:1402-1536

5. Gabriel, S. E., Dennis, R. D., John, L. E. and Leonard, J. P. (2011): "Pillar and Roof Span Design Guidelines for Underground Stone Mines." Department of Health and Human Services (NIOSH) Pittsburgh, Publication No. 2011–171.

6. Kvapil, R. and Blake, W. (1973): "Geometry and stability determination of large dimension Cut and Fill rooms at Kamoto." Proceedings of the Jublee Symposium on Mine Filling. pp-147-154.

7. Moshab (1997): "Geotechnical considerations in underground mines (Guidelines)." Mines Occupational Safety and Health Advisory Board, Department of Industry and Resource, Western Australia; Document No: ZME723QT.

8. Deb, D. and Das, K. C. (2011): "Enriched finite element procedures for analyzing decoupled bolts installed in rock mass." *International Journal for Numerical and Analytical Methods in Geomechanics*. Vol. 35, No. 15, page-1636-1655.

9. Esterhuizen, G. S. and Iannacchione, A. T. (2011): "Effect of the Dip and Excavation Orientation on Roof Stability in Moderately Dipping Stone Mine Workings." Department of Health and Human Services (NIOSH) Pittsburgh.

10. Hoek, E. and Brown, E. T. (1997): "Practical estimates of rock mass strength." *International Journal of Rock Mechanics and Mining Sciences*, Vol 34, No 8, pages 1165-1186.

11. Sinha, R. K., Jawed, M. and Sengupta, S. (2015): "Influence of rock mass rating and in situ stress on stability of roof rock in bord and pillar development panels" *International Journal of Mining and Mineral Engineering*, Vol. 6, No. 3, pp- 258- 275.

GENERATION OF ELECTRICITY FROM COAL FIRE

8.0 Conclusion

There are many challenges to be faced in designing a TEG system that will operate at high temperature. Efficiency of a TEG system lies with the temperature gradient and the amount of heat flow through the units. Success of the scheme will largely depend on efficiency and heat exchange technology of the TEG system. In addition, coal fire is not always exposed on horizontal surface. Sometimes it emerges at a vertically downward level. TEG systems to be designed in such a way that they reach to these places also. Efficient storage and distribution of the electricity needs to be planned for succesful implementation of such scheme.

References

1. Mishra, R. K., Roy, P. N. S., Panday, J., Khalkho, A. and Singh, V. K. (2014): "Study of coal fire dynamics of Jharia coalfield using satellite data," *International Journal of Geomatics and Geosciences*, Vol., 4, Issue 3, March 2014, pp-477-484.

2. Singh, Anjali, Raju, Ashwani and Pitambarpati, Narendra Kumar (2017): "Mapping of coal fire in Jharia coalfield, India : remote sensing based approach," *Journal of Indian Society of Remote Sensing*, vol. 45; Issue 2, April 2017, pp 369-376.

3. Michalski, S. R., Custer, E. S. and Munshi, P. L. (1997): Investigation of the Jharia coalfield mines Fire – India, Proceedings of American Society of Mine and Reclamation, 1997, pp 221-223.

4. Bhattacharya, A. and Reddy, C. S. S. (1994): "Underground and Surface Coal Fire Detection in Indian Jharia Coalfield Using Airborne Thermal Infrared Data," *Asia-Pacific Remote Sensing Journal*, 7(1): 59-73, 1994.

5. Sensors, ISSN 1424-8220, 14; 2014.